Electron nuclear dynamics of LiH and HF in an intense laser field

J. Broeckhove,* M. D. Coutinho-Neto, E. Deumens, and Y. Öhrn
Quantum Theory Project, University of Florida, Gainesville, Florida 32611-8435
(Received 2 June 1997)

The electron nuclear dynamics theory (END) extended to include a time-dependent external field is briefly described. The dynamical equations, in addition to the full electron nuclear coupling terms, now also contain the interactions of both the nuclei and the electrons with the external field. This extended END theory is applied to the study of vibrational excitations of the simple diatomics HF and LiH. The END results using an intense infrared laser field are compared with those of molecular dynamics as well as those from quantum wave-packet calculations. While the effect of the nonadiabatic electron-nuclear coupling terms on the vibrational dynamics is negligible for the chosen application, the electron-field coupling has a significant impact. [S1050-2947(97)04412-0]

PACS number(s): 42.50.Hz

I. INTRODUCTION

The familiar Born-Oppenheimer approximation leads to a two-tiered approach of molecular dynamics. First the electronic potential energy surfaces—and perhaps coupling matrix elements—are calculated and subsequently the nuclear motion is studied on the electronic potentials. The aim of the electron nuclear dynamics (END) theory is to provide a full description of molecules as systems of interacting electrons and nuclei. It is comprehensive in that it considers all the constituent particles of the system at once and thus bypasses the calculation of electronic potentials and couplings. It is also comprehensive in that it allows for a hierarchy of approximations with increasingly sophisticated descriptions of the system, from classical to quantum for the nuclei, from single to multiple configuration determinants for the electrons.

END theory has been extensively reviewed (see, e.g., Deumens *et al.* [1]). The dynamical END equations are determined using the principle of least action. The choice of the variational electron-nuclear wave function including the basis set is the only approximation. At the lowest level one usually considers highly localized nuclear wave packets or classical nuclei, retaining the electron-nuclear coupling terms. The electrons are described by a single complex, spin unrestricted Thouless [2] determinantal wave function. The total molecular wave function is diabatic in nature. This leads to Hamiltonian equations of motion that describe the time evolution of the system as trajectories in the generalized phase space whose coordinates are the average nuclear positions and momenta and the complex Thouless orbital parameters for the electrons. The latter are related to more standard molecular orbital coefficients via a general unitary transformation. Integration of this set of coupled first-order differential equations in time from a given set of initial conditions produce END trajectories. Such trajectories depict the classical paths of the nuclei as well as the distribution of electronic charge; in short, the time evolution of the variational wave function, and hence any expectation value calculated with it. This simplest level of END theory provides an intuitively simple and appealing picture of the dynamics of a molecular system. Higher-order approximations may be derived by invoking more sophisticated variational wave functions. Equations of motion have been derived with multiconfigurational wave functions for the electrons [3], and delocalized states for the nuclei have also been considered [4].

The Hamiltonian that generates the trajectories, i.e., the generator of infinitesimal time translations in the generalized phase space, is simply the expectation value of the quantum Hamiltonian of the molecule with respect to the variational wave function. Familiar terms such as electronic energy and nuclear kinetic energy can be discerned in its expression. In this paper we show that the equations of motion are modified in a straightforward manner when the Hamiltonian includes interaction with a time-dependent electric field. Coupling of both electrons and nuclei to the field shows up as additional forces.

In previous END work, vibrational dynamics in H_2O was investigated by distorting the initial molecular geometry. Frequency analyses of the ensuing nuclear motion with the Prony method then yielded values for the bending and stretching modes [5]. Using the same Prony method of analysis, the vibrational frequencies excited in a H_2 target after collision with H^+ have been studied [6,7]. In the present study we look at vibrational excitation through the interaction with intense infrared laser fields. Approximations appropriate to intense lasers are introduced, namely, treating the field classically, and employing the dipole approximation. Thus the molecule interaction with laser light can be formulated in terms of a time-dependent external field. This formulation is not restricted to harmonic time dependence, but is general.

Excitation induced through intense infrared lasers in the HF molecule has been studied extensively. Both nonrotating [8] and rotating HF [9,10] in a monochromatic field have been considered and the quantum and classical approaches compared and found to lead to similar conclusions. Classical mechanics predicts time-averaged quantities of the correct

*Permanent address: Department of Mathematics and Computer Science, University of Antwerp (RUCA), Groenenborgerlaan 171 B2020, Antwerpen, Belgium.

order of magnitude and also correctly predicts increased, although underestimated, excitation for laser frequencies to the red of the fundamental one-photon resonance. It does not produce peaks at the multiphoton frequencies. This can be understood since the multiphoton resonances are essentially quantal phenomena. The anharmonicity of molecular vibrations impedes the efficiency of the excitation process because the field becomes more off-resonant up the ladder of excited states and the dipole transition matrix elements diminish progressively. Efforts have been made to tailor the laser field such that excitation or dissociation probabilities are optimal. Investigations have been done with two-mode lasers [11–13], with chirped ultrashort pulses [14], with trains of pulses [15], and also with the use of control theory to optimize the features of the pulse trains [16].

In view of this previous work, little needs to be added concerning the interrelation of classical and quantum description of the laser or the effect of the laser properties on the nuclear vibrational excitation. Our study focuses on the impact of the coupling to the electrons, either directly through the nonadiabatic electron-nuclear terms or indirectly through the effect of the electron-field interaction on the electronic structure. In all of the above-mentioned investigations it is assumed that the electronic structure is not perturbed by the electron-field coupling even though extremely high (10^{12}–10^{14} W/cm^2) power densities are used. Our method allows us to take a critical look at this assumption. We show that, in the cases studied, the nonadiabatic terms have negligible effect, while the modification of the electronic structure engendered by the interaction with the field has considerable effect on the vibrational dynamics. Other dynamics studies have been made with external fields and approximate (diatomics in molecules, DIM) surfaces (see, e.g., [17]) taking into account nonadiabatic effects.

We consider the simple diatomic molecules HF and LiH and initial conditions that do not induce rotation as a first effort, for computational simplicity and because diatoms allow for a stringent comparison of the END approach with quantum wave-packet calculations. Particularly the HF system has been used extensively in various studies.

These two diatomics are quite different. LiH has a bigger dipole, is a strongly ionic molecule even for large nuclear displacements, and has a rather anharmonic potential, while HF is more harmonic and has a nonlinear dipole as a function of internuclear distance indicating a more covalent bonding character.

II. THEORETICAL BACKGROUND

The key element of END is the quantum time-dependent variational principle (TDVP) which states that the quantum action integral

$$A=\int dt\langle\zeta|i\frac{\partial}{\partial t}-H|\zeta\rangle/\langle\zeta|\zeta\rangle \tag{1}$$

should be made stationary. Variation of the wave function $|\zeta\rangle$ over the entire state space yields the time-dependent Schrödinger equation, while variation over a subspace yields the TDVP approximation for time evolution over that subspace. Using a coherent state manifold as a variational subspace has significant advantages [18,1]. The parametrization of the wave function defines a generalized phase space with the coherent state parameters as coordinates and the TDVP leads to a system of Hamiltonian equations of motion.

The END ansatz for the variational wave function is a molecular coherent state

$$|\zeta\rangle=|\mathbf{z},\mathbf{R}\rangle|\mathbf{R},\mathbf{P}\rangle\equiv|z\rangle|\phi\rangle, \tag{2}$$

where the electronic part is a single determinantal (unnormalized) coherent state

$$|z\rangle=\det\{\chi_i(x_j)\}, \tag{3}$$

in terms of the nonorthogonal spin orbitals $\chi_i=u_i+\sum_{j=N+1}^{K}u_jz_{ji}$ expressed in terms of a basis $\{u_i\}$ of atomic Gaussian type orbitals of rank K centered on the dynamically moving nuclei and with complex coefficients $\{z_{ji}\}$. The nuclear part is represented by localized Gaussians

$$|\phi\rangle=\prod_k \exp\left[-\frac{1}{2}\left(\frac{X_k-R_k}{b}\right)^2+iP_k(X_k-R_k)\right] \tag{4}$$

or, in the narrow wave-packet limit, by classical trajectories (R_k,P_k). The equations of motion obtained from this ansatz are

$$\begin{bmatrix} i\mathbf{C} & \mathbf{0} & i\mathbf{C}_\mathbf{R} & \mathbf{0} \\ \mathbf{0} & -i\mathbf{C}^* & -i\mathbf{C}_\mathbf{R}^* & \mathbf{0} \\ i\mathbf{C}_\mathbf{R}^\dagger & -i\mathbf{C}_\mathbf{R}^T & C_{\mathbf{RR}} & -\mathbf{I} \\ \mathbf{0} & \mathbf{0} & \mathbf{I} & \mathbf{0} \end{bmatrix}\begin{bmatrix} \dot{\mathbf{z}} \\ \dot{\mathbf{z}}^* \\ \dot{\mathbf{R}} \\ \dot{\mathbf{P}} \end{bmatrix}=\begin{bmatrix} \partial E/\partial\mathbf{z}^* \\ \partial E/\partial\mathbf{z} \\ \partial E/\partial\mathbf{R} \\ \partial E/\partial\mathbf{P} \end{bmatrix}, \tag{5}$$

where the dot represents time differentiation, E is the expectation value of the quantum Hamiltonian, and where the dynamical metric contains the various coupling terms

$$\mathbf{C}=\left.\frac{\partial^2\ln S(\mathbf{z}^*,\mathbf{R}',\mathbf{z},\mathbf{R})}{\partial\mathbf{z}^*\partial\mathbf{z}}\right|_{\mathbf{R}'=\mathbf{R}}, \tag{6}$$

$$\mathbf{C}_\mathbf{R}=\left.\frac{\partial^2\ln S(\mathbf{z}^*,\mathbf{R}',\mathbf{z},\mathbf{R})}{\partial\mathbf{z}^*\partial\mathbf{R}}\right|_{\mathbf{R}'=\mathbf{R}}, \tag{7}$$

and

$$\mathbf{C}_{\mathbf{RR}}=-2\,\mathrm{Im}\left.\frac{\partial^2\,\ln S(\mathbf{z}^*,\mathbf{R}',\mathbf{z},\mathbf{R})}{\partial\mathbf{R}'\partial\mathbf{R}}\right|_{\mathbf{R}'=\mathbf{R}}, \tag{8}$$

with $S(\mathbf{z}^*,\mathbf{R}',\mathbf{z},\mathbf{R})=\langle\mathbf{z},\mathbf{R}'|\mathbf{z},\mathbf{R}\rangle$.

The Hamiltonian

$$H=\sum_A\frac{P_A^2}{2M_A}+\frac{1}{2}\sum_{A,B}\frac{Z_AZ_B}{r_{A,B}}+\sum_{A,i}\frac{Z_A}{r_{A,i}}+\sum_i\frac{P_i^2}{2m_e}+\frac{1}{2}\sum_{i,j}\frac{1}{r_{i,j}}+\left(\sum_A Z_A\vec{r}_A+\sum_i e\vec{r}_i\right)\cdot\vec{\varepsilon}, \tag{9}$$

with the external field interaction has sums over nuclei (A and B) and over electrons (i and j). The $\vec{\varepsilon}=\vec{\varepsilon}(t)$ is the classical electric field representing the laser light. The energy in the equations of motion Eq. (5) is given by

$$E=\sum_A \frac{P_A^2}{2M_A}+E_{\rm el}(z,z^*,R)+[\vec{\mu}_n(R)+\vec{\mu}_{\rm el}(z,z^*,R)]\cdot\vec{\varepsilon}, \tag{10}$$

with $E_{\rm el}$ the expectation value of the electronic Hamiltonian.

A. Molecular dynamics

The END equations (5) reduce to those of molecular dynamics (MD) on a potential energy surface, when $\dot{z}=0$, for all z coefficients. Then

$$\frac{\partial E(z,z^*,R,P,\vec{\varepsilon})}{\partial z^*}=iC_R\dot{R} \tag{11}$$

and

$$\begin{bmatrix}\mathbf{C_{RR}} & -\mathbf{I}\\ \mathbf{I} & \mathbf{0}\end{bmatrix}\begin{bmatrix}\dot{\mathbf{R}}\\ \dot{\mathbf{P}}\end{bmatrix}=\begin{bmatrix}\partial E/\partial\mathbf{R}\\ \partial E/\partial\mathbf{P}\end{bmatrix}. \tag{12}$$

A bit more explicitly the first equation becomes

$$\frac{\partial E_{\rm el}(z,z^*,R)}{\partial z^*}+\frac{\partial\vec{\mu}_{\rm el}(z,z^*,R)}{\partial z^*}\cdot\vec{\varepsilon}=iC_R\dot{R} \tag{13}$$

the solutions of which are the electronic dynamical variables $z_s=z_s(R,\dot{R},\vec{\varepsilon})$. This solution then defines the forces exerted on the nuclei in the second equation. This set of equations is analogous to the familiar molecular dynamics approach to motion on a self-consistent-field (SCF) potential energy surface. There are, however, some differences. It can be shown [1] that for $\vec{\varepsilon}=\vec{0}$ Eq. (13) amounts to SCF with properly boosted molecular orbitals and a similarly boosted electronic energy. This formulation constitutes an alternative to the more traditional use of electron translation factors to describe the dragging of the electrons by the nuclei. If the velocity-dependent terms are neglected in Eqs. (11) and (12) the formulation of classical nuclear motion on a Born-Oppenheimer potential surface is recovered. In our case there is also an explicit field dependence in the equation for the electronic structure. For strong fields the electronic orbitals are modified and this in turn has an effect on forces driving the nuclei. We show how this effect may be analyzed in terms of the electronic polarizability.

We also employ molecular dynamics (MD) without the dipole term in Eq. (13), but retaining it in Eq. (12), and label that the nonpolarized (MD-NP) approach. This is more in line with traditional methods that use classical nuclei on field-independent potentials.

B. Wave-packet propagation

We also perform quantum wave-packet (WP) calculations using the split operator propagation method [19]. The time-dependent Schrödinger equation is solved by applying the time evolution operator to the initial state

$$\Psi(t)=U(t,t_0)\Psi(t_0). \tag{14}$$

U is defined as

$$U(t,t_0)=\boldsymbol{\tau}\left\{\exp\left[-i\int_{t_0}^{t}dsH(s)\right]\right\} \tag{15}$$

using the Dyson time-ordering operator $\boldsymbol{\tau}$, which is required by the presence of a time-dependent potential in the Hamiltonian. The propagation interval from t_0 to t is subdivided into short time steps $\boldsymbol{\epsilon}$,

$$U(t,t_0)=\prod_{j=1}^{j=N}U(t_j,t_{j-1}),\quad t-t_0=N\boldsymbol{\epsilon},\quad t_j=t_0+j\boldsymbol{\epsilon} \tag{16}$$

and the evolution operator for each such step is approximated by

$$U(t+\boldsymbol{\epsilon},t)=\exp\left(-i\,\frac{\boldsymbol{\epsilon}}{2}\,T\right)\exp\left(-i\int_t^{t+\boldsymbol{\epsilon}}ds\;V(s)\right)\times\exp\left(-i\,\frac{\boldsymbol{\epsilon}}{2}\,T\right). \tag{17}$$

The power of the algorithm lies in this particular factorization. The action of the potential energy V is evaluated while the wave function is in the coordinate representation, i.e., defined by its values on a grid in coordinate space, while the action of the kinetic energy T is effectuated in the momentum representation using the discrete Fourier transform associated with the grid. The kinetic energy operator is multiplicative in that representation, so its action is also easily evaluated. Afterwards one transforms the wave function back to the coordinate representation with an inverse Fourier transform. This is a viable approach because of the availability of fast Fourier transform algorithms that perform these transformations very efficiently. The decomposition outlined in the above formula, including the elimination of the time-ordering operator, is correct through second order in $\boldsymbol{\epsilon}$ provided the potential has a well-behaved time dependence [20].

The Hamiltonian for the wave-packet propagation $H=T+V(t)$ has a potential

$$V(t)=V_{\rm SCF}(R)+\vec{\mu}_{\rm SCF}(R)\cdot\vec{\varepsilon}(t). \tag{18}$$

The potential and dipole are obtained from SCF calculations at several bond distances R with the END determinantal wave function using the same basis. This provides for a consistent comparison of the results between the various methods.

III. RESULTS AND DISCUSSION

A 3–21G electronic basis[a] is used in the END ansatz for both LiH and HF. This limited basis provides an acceptable model for seeking an understanding of the factors determining the dynamics. Obviously further work is needed with careful basis set studies, however, in other applications of this level of END theory we have observed a surprising insensitivity of results to basis set augmentations [21].

Because the spin symmetry of the ansatz does not break either for the MD or the MD-NP calculations, restricted Hartree-Fock (RHF) limiting behavior exists at large bond distances in the potential and dipole used in the MD and

[a]Contractions used: H:$(3s)/[2s]$, Li:$(6s,3p)/[3s,2p]$, and F: $(6s,3p)/[3s,2p]$.

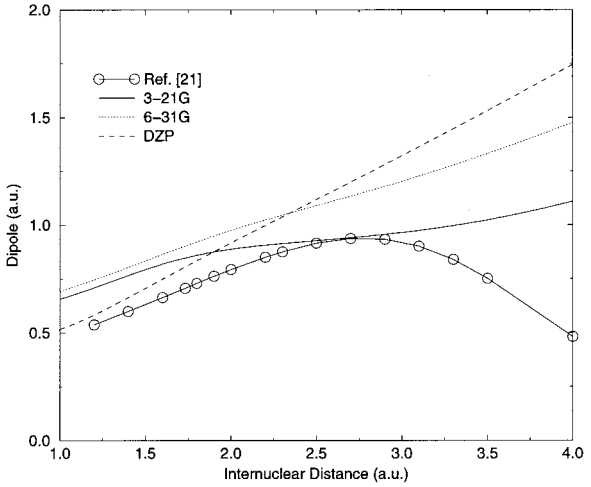

FIG. 1. Dipole moment functions for HF calculated using RHF for different basis functions (this work) and CASSCF-MRCI [22].

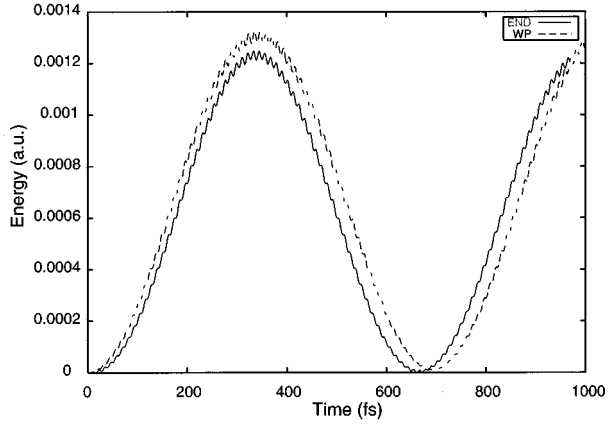

FIG. 2. Absorbed energy for LiH using a continuous field of intensity of 35.1 GW/cm^2 and a detuning of 212×10^{-6} a.u.

MD-NP wave-packet calculations. Fortunately this unphysical behavior does not affect the dynamics significantly since such large bond distances are not explored by the nuclei. The wave-packet calculations may be more susceptible to the ill-behaved region of the dipole and the potential due to the fact that the nuclear wave function has a finite width.

Unlike MD and MD-NP, the full END approach admits a consistent exploration of symmetry broken solutions that, for instance, allows for a correct description of bond breaking and bond formation in closed shell systems [21]. The agreement between the END and the MD calculations is an indication that the dynamics is not affected by the unphysical RHF behavior of the potential curve at large separation.

Another way of viewing this is that the END equations permit the ordinary differential equation solver to sample also symmetry broken solutions. Actually, in practice the solutions being generated are always of the symmetry broken type and can lead to correct dissociation limits. The details of the numerical analysis of this are outside the scope of this paper and are planned to be published as a separate study.

As a way to judge the quality of the basis set we performed time-independent calculations on HF and LiH. Results for HF show that the dipole function is somewhat sensitive to the basis set, but for the region of interest the agreement with the result obtained with a more flexible wave function [22] is acceptable (see Fig. 1). Equivalent results were obtained for LiH by Butalib and Gadéa [23] using full configuration interaction (the dipole moment results were obtained from Berriche and Gadéa [24]). Values obtained for the equilibrium distance are 1.771 a.u. for HF and that for the vibrational frequency is 4150.8 cm^{-1}, while for LiH we calculate 3.066 a.u. and 1428.8 cm^{-1}, respectively.

The models defined by the 3–21G bases are adequate for our purposes. However, it should be pointed out that an important quantity in the analysis of the time-independent MD-NP calculations is the force term $\vec{\varepsilon}\cdot\partial\vec{\mu}/\partial R$. For LiH using the 3–21G basis this term is almost a factor 2 greater than the one obtained from more exact calculations, while for HF it is too small, particularly around $R=2.0$ a.u.

The laser field is written as

$$\vec{\varepsilon}(t)=\vec{\varepsilon}_0 p_\varepsilon(t)\sin(\Omega t), \tag{19}$$

where $\vec{\varepsilon}_0$ defines the electric field strength and polarization, p_ε is a dimensionless function with maximum value 1.0 describing the pulse shape, and Ω is the carrier frequency. Two field intensities, each with linear polarization, are used, 35 GW/cm^2 and 1 TW/cm^2 corresponding to field strengths of 0.001 and 0.0054 a.u., respectively. In combination with the initial condition that aligns the molecule with the field this avoids introducing any rotational motion; a realistic assumption, since rotational time scales are much longer than vibrational ones and we do not want to evolve the system over a long time anyway. The quantum wave-packet propagation is similarly limited to the vibrational degree of freedom. The END initial conditions are further specified by using the nuclear equilibrium distance and putting the electrons in the SCF state at that geometry. The initial condition for the quantum evolution is the ground vibrational state of the SCF potential. It is calculated using the renormalized Numerov method [25].

In the zeroth-order approximation the system may be considered to be a linearly driven harmonic oscillator, i.e., the potential is assumed harmonic and the dipole linear, while the electrons have no couplings to the nuclear dynamics. This approximation is appropriate and interesting because the classical and quantum response of a harmonic oscillator to a linear external force is identical [26]. The energy of the oscillator system with mass m and frequency ω, initially in its ground state, is given by

$$\epsilon(t)=\frac{\mu_0^2E_0^2}{2m}\left|\int_0^t ds\; p_\varepsilon(s)\exp[i\omega s]\right|^2. \tag{20}$$

For a continuous-wave monochromatic field, i.e., $p_\epsilon=1$, and small detuning $\Delta=\Omega-\omega$, the energy transfer is periodic with the detuning period $2\pi/\Delta$,

$$\epsilon(t)=\frac{\mu_0^2E_0^2}{2m\Delta^2}\sin^2\left(\frac{\Delta}{2}t\right). \tag{21}$$

An example for LiH of the absorbed energy for a continuous-wave field is shown in Fig. 2 obtained both with

TABLE I. Average absorbed energy (in 10^{-3} a.u.) taken over the first detuning period for LiH using a continuous field with intensities 35.1 GW/cm^2 (upper part of the table) and 1 TW/cm^2 (lower part of the table) at different detunings Δ (in 10^{-6} a.u.).

Δ	END	MD	WP
212	0.59	0.60	0.61
−68	4.81	4.63	5.45
−248	0.56	0.56	0.72
212	5.84	5.87	6.87
−68	10.97	11.06	12.29
−248	14.55	14.53	15.38

the END and the quantum wave-packet methods. The results are for matching detuning, rather than identical field frequency, because the END and the quantum methods have slightly different fundamental frequencies ω. We have simply used the ground state for both the classical and the quantum case, and have not averaged over ensembles of trajectories to improve the classical-quantum correspondence for the initial condition. For a ground state in a nearly harmonic system this should be an acceptable approximation. In this example we have used the LiH molecule. The weaker field, and a detuning above the fundamental frequency, i.e., away from multiphoton resonances, conspire to optimize oscillatorlike behavior and the mutual agreement between the methods. Considerable differences do occur for other field conditions, but for a detailed investigation we refer to Walker and Preston [8], Dardi and Gray [9], Lin *et al.* [27], and Goggin and Milonni [28].

Time-averaged absorbed energies [8,9,27] are used to compare the classical and the quantum calculations. Averages were taken over detuning period intervals. The spectrum of average absorbed energy as a function of field frequency is a broad peak with spikes at the multiphoton frequencies. The broad peak is reproduced in calculations with classical treatment of the nuclei, but the evidence of multiphoton frequencies is inherently quantum mechanical. As the field strength increases the peak heightens and shifts to the red. This is apparent in the results in Table I, which gives the average absorbed energy for LiH. The stronger field shows the larger absorption values at detunings that are shifted to the red.

As expected from the literature both END and MD exhibit agreement with the quantum wave-packet results. None of the detunings in Table I coincide with a multiphoton frequency. The differences between END and MD in Table I appear to be almost negligible. A similar observation was made when inspecting results for the time evolution of bond distance and electric dipole moment. The same observation was again made for the differences between END and MD in all test calculations on HF. This leads us to the first conclusion, namely, that for the kind and magnitudes of time-dependent field used here, nonadiabatic effects in the molecular Hamiltonian are of little consequence for the dynamics. Since the MD calculations require significantly less computational time, the remaining calculations are all of this type.

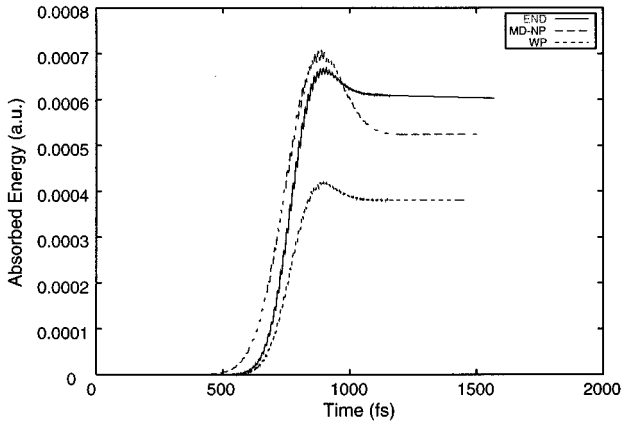

FIG. 3. Absorbed energy as a function of time for LiH with the END, MD-NP, and WP calculations. A pulsed field with intensity 35.1 GW/cm^2 and detuning -248×10^{-6} a.u. is used.

For a pulsed field of finite duration one can compute the energy absorbed after the pulse has subsided. To a very good approximation this also applies to a pulse with a Gaussian profile of width τ (full width at half maximum) and one finds

$$\epsilon(\infty)=\frac{\mu_0^2\varepsilon_0^2}{2m\Delta^2}\,\frac{\pi}{4}\,(\Delta\tau)^2\exp[-(\Delta\tau)^2]. \tag{22}$$

The pulse duration needs to be matched to the detuning Δ of the carrier frequency to obtain optimum energy absorption. When the pulse is too short the system does not have enough time to respond; when the pulse is too long as in Fig. 3, the system releases energy back to the field. We have used a width of 5942 a.u., which roughly matches the larger negative detuning (-248×10^{-3}). An example of the time evolution of the absorbed energy is shown in Fig. 3 for LiH.

Focusing on the effect of the polarizability we consider Figs. 4 and 5. A comparison is shown of the final absorbed energy for LiH and HF with the MD and MD-NP approximations, i.e., with and without polarizability of the system. Results for the lower field intensity show comparable differ-

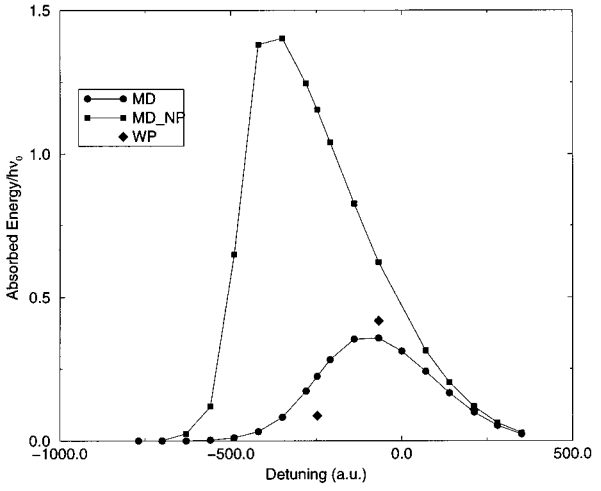

FIG. 4. Absorbed energy, in $h\nu_0$ units, as a function of detuning (in 10^{-6} a.u.) for HF calculated with MD and MD-NP.

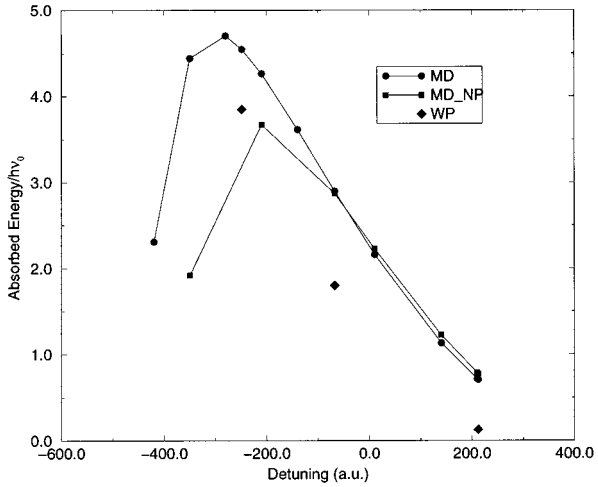

FIG. 5. Absorbed energy, in $h\nu_0$ units, as a function of detuning (in 10^{-6} a.u.) for LiH calculated with MD and MD-NP.

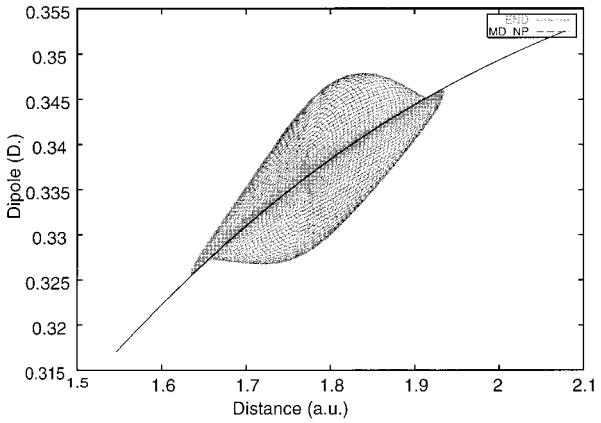

FIG. 7. Molecular dipole vs bond distance traced during time evolution for HF at detuning -68×10^{-6} a.u. and field intensity of 1.0 TW/cm^2 for MD-NP (line) and MD (oscillatory parametric curve). The calculated equilibrium bond distance is 1.771 a.u.

ences between MD and MD-NP on both LiH and HF with the maximum absorption frequency being closer to the harmonic frequency (zero detuning).

It is immediately evident that the effect of the polarizability is significantly more pronounced for HF than for LiH. This is also illustrated in Figs. 6 and 7 for specific detunings.

The use of different approximations to solve the dynamics, of course, leads to different approximations for the description of the time-dependent dipole. More precisely, MD introduces relaxation with the field and adiabatic corrections and END also introduces nonadiabatic corrections.

As already mentioned, the dynamics produced by END and MD are here very similar. This similarity is assigned to the very small nonadiabatic effects [i.e., C_R terms in Eq. (5)] on the dynamics. In contrast, the MD dynamics is different from the MD-NP, indicating that electronic relaxations, or polarization with the field is an important dynamical effect. The polarization is shown in Figs. 6 and 7 as the departure from the MD-NP dipole function given by the solid diagonal line. Note how the amplitude of the motion is much smaller in MD for HF, suggesting a more important role of the polarizability for this molecule.

The response of the dipole moment to the field allows estimates of the polarizability and hyperpolarizabilities to be made. The dynamics explicitly yields the dipole at each time step, allowing the dipole to be obtained directly from the time-dependent dipole (see Fig. 8) as a function of the field for different internuclear distances.

If we assume a linear response of the dipole with the field, $\vec{\mu}=\vec{\mu}_0+\alpha\vec{\varepsilon}(t)$, the dependence of the polarizability (α_{xx} in this case) on the internuclear distance is obtained directly from the data in Fig. 8 to produce the results in Fig. 9. Similar results are computed for LiH and shown in Fig. 10. Computed values for HF at equilibrium are similar to other results in the literature [29] using larger basis sets.

The computed polarizability is not exactly the dynamic one since it represents the response to a Gaussian shaped pulse with a frequency spread. Calculations [30] using our basis sets for static polarizabilities at different internuclear distances have shown that the variation with frequency is

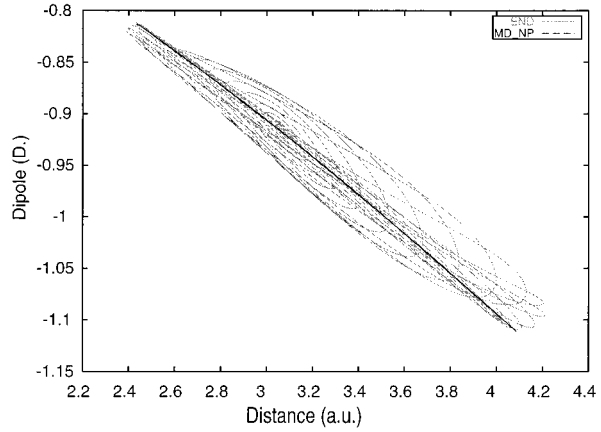

FIG. 6. Molecular dipole vs bond distance traced during time evolution for LiH at detuning -68×10^{-6} a.u. and field intensity of 1.0 TW/cm^2 for MD-NP (line) and MD (oscillatory parametric curve). The calculated equilibrium bond distance is 3.066 a.u.

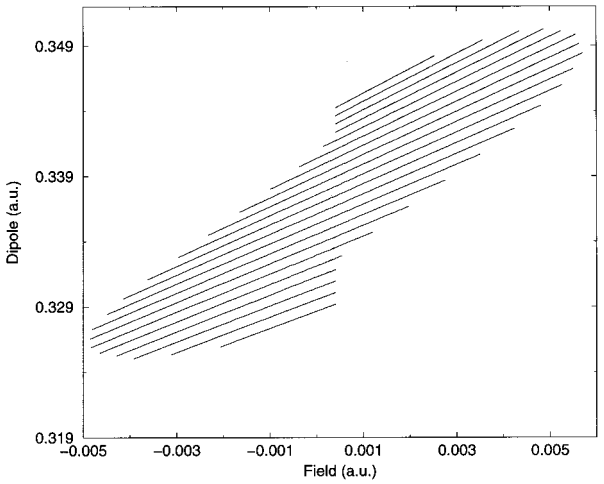

FIG. 8. Dipole as a function of the field for HF for different internuclear distances (different lines). The field intensity used is 1 TW/cm^2 and the detuning is 248×10^{-3} a.u.

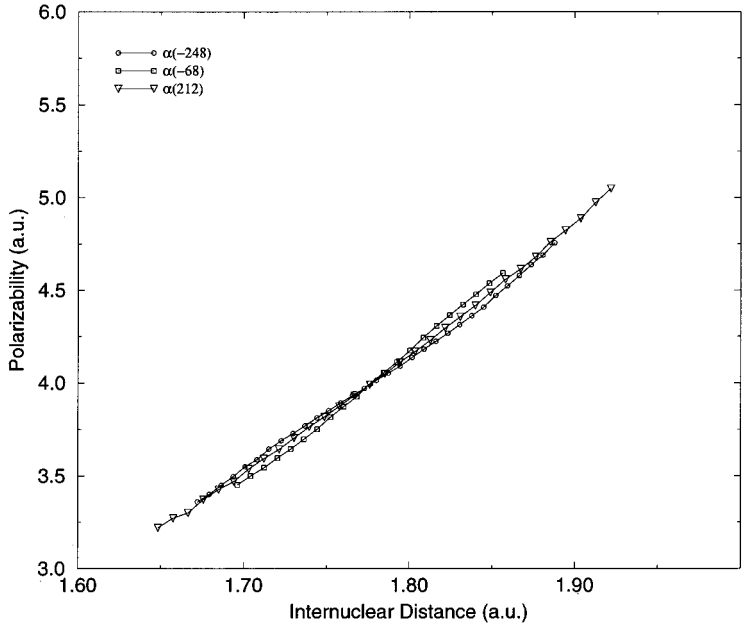

FIG. 9. Polarizability $[\alpha(\Delta)]$ vs internuclear distance for HF using a field of 1 TW/cm^2 and different detunings.

small, but bigger for LiH, and fluctuates about the value for the static polarizability for both LiH and HF.

The effect of the polarizability on the dynamics of the two systems may be discussed in terms of classical perturbation theory [31]. The classical analog for a polarizable molecular system is that of an anharmonic oscillator driven by a force of frequency Ω, arising from the dipole interaction, and a force with frequency 2Ω, arising from the polarizability [the polarizability α accounts for a contribution to the energy which can be expressed as $-\frac{1}{2}\alpha(R)\varepsilon_0^2(t)p_\varepsilon\cos^2(\Omega t)$]. It can be shown that an anharmonic oscillator driven by a force of frequency close to $2\omega_0$ undergoes resonance. Assuming validity of perturbation theory the equation of motion for such a system reduces to that of an anharmonic oscillator driven by an effective force with frequency Ω and proportional to the original force, the anharmonicity, and the amplitude of the motion. For LiH and HF the derivative $\partial\alpha(R)/\partial R$ is always positive while the anharmonic coefficient is negative, making the sign of the effective force opposite to the sign of the field. The result is an enhancement of the dipole force term for LiH (which also has a different sign with respect to the field) and a reduction of the dipole force for HF.

IV. CONCLUSIONS

The electron nuclear dynamics theory which is capable of full nonadiabatic treatment of molecular systems has been applied to study molecular processes in a time-dependent external field. In this initial study we have investigated the effects of nonadiabatic coupling terms, as well as the interaction of intense laser fields with the electron and the nuclear dynamics for the simple diatomic molecules LiH and HF. At

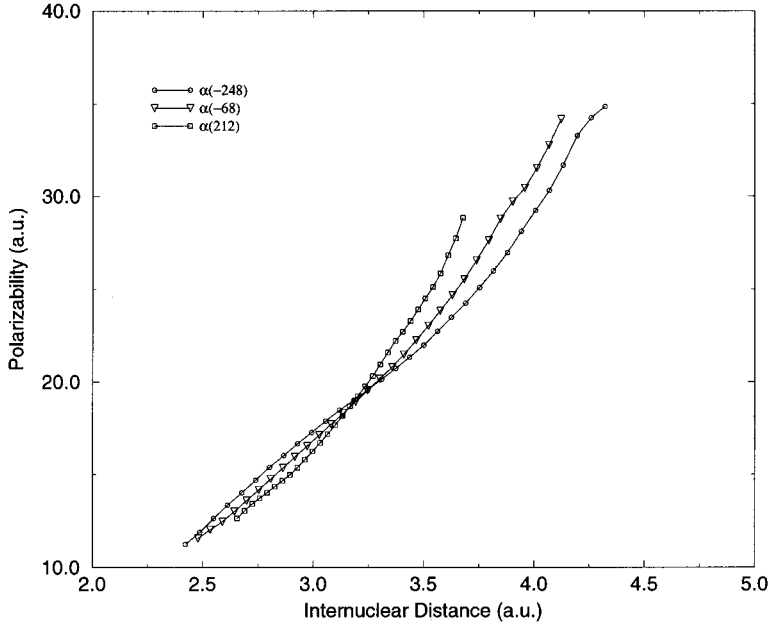

FIG. 10. Polarizability $[\alpha(\Delta)]$ vs internuclear distance for LiH using a field of 1 TW/cm^2 and different detunings.

the chosen field intensities the results of the full END and the molecular dynamics on a field-dependent potential energy surface yield similar results, the difference being greater for the HF molecule. This indicates that for the cases studied the infrared (IR) light absorption is adiabatic.

The applied field can be considered of moderate intensity, however, in view of the absorbed energy (as seen in Figs. 4 and 5) and the number of vibrational quanta involved, the situations are quite different for the two molecules.

The external field interaction with the electrons appears to be crucial for the correct description of the dynamics, since inclusion of the polarization proves to have a substantial effect. The polarization effects are more pronounced for the HF molecule than for LiH.

The new capability of the END approach to molecular processes offers interesting possibilities to study more complex molecular systems. Such work is in progress.

ACKNOWLEDGMENTS

We gratefully acknowledge support from the U.S. Office of Naval Research. One of us (M.D.) acknowledges support from CAPES. Calculations have been performed at the J. C. Slater Computing Facility. The authors acknowledge the sponsors that have made this facility possible, in particular, the IBM Corporation through its SUR 1996 program (University of Florida). We thank H. Berriche and F. X. Gadéa for supplying us with their unpublished dipole moment results for LiH.

[1] E. Deumens, A. Diz, R. Longo, and Y. Öhrn, Rev. Mod. Phys. **66**, 917 (1994).
[2] D. J. Thouless, Nucl. Phys. **21**, 225 (1960).
[3] E. Deumens, Y. Öhrn, and B. Weiner, J. Math. Phys. **32**, 1166 (1991).
[4] E. Deumens and Y. Öhrn, J. Phys. Chem. **92**, 3181 (1988).
[5] E. Deumens, A. Diz, H. Taylor, and Y. Öhrn, J. Chem. Phys. **96**, 6820 (1992).
[6] R. Longo, E. Deumens, and Y. Öhrn, J. Chem. Phys. **99**, 4554 (1993).
[7] J. A. Morales, A. C. Diz, E. Deumens, and Y. Öhrn, Chem. Phys. Lett. **233**, 392 (1995).
[8] R. B. Walker and R. K. Preston, J. Chem. Phys. **67**, 2017 (1977).
[9] P. S. Dardi and S. K. Gray, J. Chem. Phys. **77**, 1345 (1982).
[10] F. J. Lin and J. T. Muckerman, Comput. Phys. Commun. **63**, 538 (1991).
[11] J. R. Stine and D. W. Noid, Opt. Commun. **31**, 161 (1979).
[12] G. Jolicard and G. D. Billing, J. Chem. Phys. **90**, 346 (1989).
[13] A. Guldberg and G. D. Billing, Chem. Phys. Lett. **186**, 229 (1991).
[14] S. Chelkowski, A. D. Bandrauk, and P. B. Corkum, Phys. Rev. Lett. **65**, 2355 (1990).
[15] B. G. Dibble and R. B. Shirts, J. Chem. Phys. **94**, 3451 (1991).
[16] M. Kaluza, J. T. Muckerman, P. Gross, and H. Rabitz, J. Chem. Phys. **100**, 4211 (1994).
[17] A. Bastida and F. X. Gadéa, Z. Phys. D **39**, 325 (1997).
[18] P. Kramer and M. Saraceno, *Geometry of the Time-Dependent Variational Principle in Quantum Mechanics* (Springer, New York, 1981).
[19] M. D. Feit, J. A. Fleck, Jr., and A. Steiger J. Comput. Phys. **47**, 412 (1982).
[20] J. A. Fleck, J. R. Morris, and M. D. Feit, J. Appl. Phys. **10**, 129 (1976).
[21] Y. Öhrn, J. Oreiro, and E. Deumens, Int. J. Quantum Chem. **58**, 583 (1996).
[22] W. T. Zemke, W. C. Stwalley, S. R. Langhoff, G. L. V. Aldemara, and M. Berry, J. Chem. Phys. **95**, 7846 (1991).
[23] A. Butalib and F. X. Gadéa, J. Chem. Phys. **97**, 1144 (1992).
[24] H. Berriche and F. X. Gadéa (private communication).
[25] B. R. Johnson, J. Chem. Phys. **67**, 4086 (1977).
[26] R. J. Glauber, Phys. Rev. Lett. **10**, 84 (1963).
[27] J. Lin, P. Jones, J. Guckert, and E. I. Solomon, J. Am. Chem. Soc. **113**, 8312 (1991).
[28] M. E. Goggin and P. W. Milonni, Phys. Rev. A **37**, 796 (1988).
[29] H. Sekino and R. J. Bartlett, J. Chem. Phys. **84**, 2726 (1986).
[30] B. Champagne and D. Jacquemin (private communication).
[31] L. D. Landau and E. M. Lifshitz, *Mechanics* (Pergamon, New York, 1976).